



ESTIMATION OF THE MAXIMUM BENDING MOMENT OF CANTILEVER SHEET PILE WALLS BY USING MULTIPLE LINEAR REGRESSION ANALYSIS

Recep AKAN*

Süleyman Demirel University, Faculty of Engineering, Department of Civil Engineering, Isparta, TURKEY

Keywords

*Cantilever Sheet Pile,
Bending Moment,
Multiple Linear Regression,
Prediction,
Sand.*

Abstract

Sheet pile walls are flexible retaining structures that are used to hold the horizontal soil pressures behind them, especially in situations that cause stress changes such as excavation. They are divided into two as cantilever and externally supported. Cantilever walls are used in excavations with a maximum depth of 6 meters and are supported by anchors in excavations deeper than this. Some of the values to be calculated in the design of cantilever sheet pile walls are the embedment depth and the maximum bending moment that (M_{max}) will occur in the cross-section of the wall. There are various approaches in analytical methods that have complex calculation steps such as determining earth pressures, solving second and third-order equations. In this study, the M_{max} that will occur in the cross-section of a cantilever sheet pile wall penetrates in the sand is estimated by the expressions obtained with the help of multiple linear regression (MLR) analysis. The results showed that the M_{max} may not be achieved by only MLR models but with the help of polynomial equations.

KONSOL PALPLANŞ DUVARLARIN MAKSİMUM EĞİLME MOMENTİNİN ÇOKLU LİNEER REGRESYON ANALİZİ İLE TAHMİNİ

Anahtar Kelimeler

*Konsol Palplanş,
Eğilme Momenti,
Çoklu Lineer Regresyon,
Tahmin,
Kum.*

Öz

Palplanş duvarlar, özellikle kazı gibi gerilme değişikliklerine neden olan durumlarda, yatay zemin basınçlarını arkalarında tutmak için kullanılan esnek istinat yapılarıdır. Temel olarak konsol ve dış destekli olarak ikiye ayrılırlar. Maksimum 6 metre derinliğe sahip kazılarda konsol duvarlar kullanılır ve bundan daha derin kazılarda ankrajlarla desteklenir. Konsol palplanş duvarların tasarımında hesaplanacak değerlerden bazıları gömme derinliği ve duvar kesitinde oluşacak maksimum eğilme momentidir. Toprak basınçlarının belirlenmesi ve ikinci ve üçüncü mertebeden denklemlerin çözülmesi gibi karmaşık hesaplama adımlarına sahip analitik yöntemler için çeşitli yaklaşımlar bulunmaktadır. Bu çalışmada, yapılacak bir kazı nedeniyle kuma gömülü bir konsol palplanş duvarın kesitinde oluşacak maksimum eğilme momenti, çoklu lineer regresyon analizi yardımıyla elde edilen ifadelerle tahmin edilmeye çalışılmıştır. Sonuçlar, sadece lineer regresyon modellerinin yardımı ile değil ancak tahmin sonuçlarının polinom ifadeler yardımıyla iyileştirilmesi sonucunda tatmin edici derecede başarılı tahmin edilebileceğini göstermiştir.

Alıntı / Cite

Akan, R., (2022). Estimation of the Maximum Bending Moment of Cantilever Sheet Pile Walls by Using Multiple Linear Regression Analysis, Journal of Engineering Sciences and Design, 10(1), 247-256.

Yazar Kimliği / Author ID (ORCID Number)

R. Akan, 0000-0002-9277-1659

Makale Süreci / Article Process

Başvuru Tarihi / Submission Date	23.09.2021
Revizyon Tarihi / Revision Date	27.10.2021
Kabul Tarihi / Accepted Date	26.11.2021
Yayın Tarihi / Published Date	23.03.2022

*İlgili yazar / Corresponding author: recepakan@hotmail.com, +90-246-211-1197

1. Introduction

The demand for deep excavation has increased as the country's population and urbanization have grown so the necessity of bearing the horizontal earth pressure issues has arisen. Sheet pile walls are commonly employed applications in geotechnical engineering as retaining structures, notably to bear lateral earth pressures produced by excavation. Sheet pile walls can also be constructed of wood, reinforced concrete but usually steel. Steel sheet pile walls have interlocking edges so they can work as a whole wall and provide water impermeability.

Sheet pile walls are used as cantilever walls or externally supported walls, depending on soil properties, excavation depth. Cantilever sheet piles are utilized for heights of up to 5 to 6 m and anchors are linked to the sheet pile walls to offer greater passive resistance by the infill for beyond. Sheet pile walls, unlike retaining walls, are generally temporary constructions that are constructed to sustain the soil mass laterally and are flexible.

For more than six decades, sheet pile walls have been a subject of study. Rowe (1951), Bransby and Milligan (1975), and Seok et al. (2001) are some of the studies that have done model studies on embedded walls. In addition, Rowe (1952) investigated the impact of several factors on flexible retaining walls, including surcharge load, anchor position, excavation level, soil type, wall flexibility, and soil pressure distribution on the flexible retaining wall.

There are many theoretical methods used to calculate the maximum bending moment (M_{max}), which are commonly obtained by the approximate method based on the Rankine earth pressure theory in current civil engineering applications. There are various approaches that empirical and semi-empirical offer more accurate estimates (Coduto, 2001; Das, 2007; Rankine, 1857). Design tables for normalized embedment depths for sheet pile walls were published by Bolton et al. (1989, 1990a, 1990b) based on undrained shear strength for cohesive soils and friction angle for non-cohesive soils. For anchored sheet pile walls embedded in sandy soils, Hagerty and Nofal (1992) produced simplified design charts for normalized embedment depth and anchor strength. The embedment depths of sheet pile walls subjected to lateral linear stresses in cohesionless soils were estimated using normalized relationships by Choudry et al. (2006) and Gajan (2011). Akan (2020), investigated the impact of the increment ratio of the theoretical depth of the wall on the maximum bending moment and anchor force of a single anchored sheet pile wall in the sand with varied internal friction angles when the groundwater level occurs.

Mishra et al. (2020), used a functional network (FN), genetic programming (GP), and group data processing approach to simulate a retaining wall (GMDH). To get an expression for the design of the reinforced concrete retaining wall, Akbay et al. (2020) and to obtain a decision diagram for retaining wall selection, Choi and Lee (2010) used regression analysis. Srivastava and Malhotra (2016) used regression analysis to estimate passive horizontal earth pressures, and Dagdeviren and Kaymak (2020) used regression analysis to obtain a pre-sizing recommendation for a T-shaped retaining wall.

Azzouz et al. (1976) develop regression equations to predict the compression index and compression ratio from classification or index data, and statistical techniques are utilized to assess and evaluate experimental data from consolidation experiments on a wide variety of undisturbed soils. These regression equations are then compared to several other comparable but more limited empirical correlations that have been reported by other researchers. Yoon and Kim (2006) use consolidation data to develop site-specific empirical correlation models to estimate the compression index of inorganic marine clay at Kwangyang new port in Korea. Regression analysis is used to make correlations in calculating compression index utilizing. Natural water content, void ratio, liquid limit, plasticity index, passing percentage, and specific gravity are among the soil characteristics utilized. Hirata et al. (1990) used multiple regression analysis to properly identify the connections between a mechanical characteristic and several physical parameters in both natural and artificially blended cohesive soils. The shear strength of soils is represented by two types of regression models. The Atterberg limit is used in the first model, whereas the Cam-Clay model is used in the second. Teymen and Mengüç (2020) evaluated the characteristics of uniaxial compressive strength (UCS), unit weight, Brazilian tensile strength, Schmidt hardness, Shore hardness, point load index, and P-wave velocity. Simple regression analysis, multiple regression analysis, artificial neural networks, adaptive neuro-fuzzy inference system, and genomic expression programming have all been used to forecast the UCS. Using several graphs, the computed UCS values were compared to the real UCS values were then compared. Adefemi and Wole (2013) used two-way analysis of variance and multiple regression analysis to analyze the findings of statistical research on the impact of compaction delays on characteristics of lime stabilized yellowish-brown lateritic soil. Yoon et al. (2015) use in-situ experimental data from a range of slope locations in South Korea to develop an estimation method for calculating saturated hydraulic conductivity of Korean weathered granite soils. Using diverse physical soil characteristics, a robust regression analysis was conducted, and an empirical solution was proposed. Abdi et al. (2018) used artificial neural networks and multiple regression analysis to predict UCS and modulus of elasticity (E) in sedimentary rocks. Rock samples from four different rock types were cored and

submitted to extensive laboratory testing for this purpose. Physical characteristics of investigated rocks such as P wave velocity, dry density, porosity, and water absorption were used as model inputs, whereas UCS and E were used as output factors to build the prediction models. Mahdiabadi and Khanlari (2019) used MLR, multiple nonlinear regression, artificial neural networks, and adaptive neuro-fuzzy inference system to predict UCS and E in calcareous mudstones of the Aghajari Formation. The point loading, block punch, and cylinder punch tests were performed on samples of calcareous mudstones. The determination coefficients (R^2), mean absolute percentage error, and variance accounted for were used to evaluate the performance of the created models. Bera et al. (2005) offer a regression study on bearing capacity of square footing on reinforced pond ash. Using all feasible regression approaches based on model test data to choose the important subset of the predictors, a power model was constructed to estimate bearing capacity of a square footing on reinforced pond ash at any settlement. Kumar et al. (2013) want to use soft computing techniques like multiple regression and artificial neural network models to forecast rock characteristics using drill bit speed, penetration rate, drill bit diameter, and equivalent sound level produced while drilling as input factors. UCS, Schmidt rebound number, dry density, P wave velocity, tensile strength, E, and porosity n were determined using a database of instances, and the prediction abilities of models were examined.

The M_{max} that will occur in the cross-section of a cantilever sheet pile wall is calculated in this work using expressions acquired from multiple linear regression (MLR) analysis, which simplifies the calculation procedure. For this aim, a cantilever sheet pile wall was driven into a sandy soil with the groundwater level at the dredge line in front and at various levels from the soil surface to the dredge line rear of the wall was modeled with the aid of Matlab R2015a. The acquired M_{max} findings are then submitted to MLR analysis using SPSS Statistics v17.0, and MLR expressions are created to estimate the M_{max} . The accuracy of the estimation is measured using the determination coefficient (R^2) and the mean absolute relative error (MARE), and the findings are encouraging.

2. Material and Method

The findings of the M_{max} were acquired by executing step-by-step MLR analysis with the assistance of SPSS Statistics v17.0, and the solutions of a total of 833 cantilever sheet pile wall models were conducted with the help of Matlab R2015a. As a next step, the acquired results from MLR equations were enhanced with polynomial functions. Established regression models and improved models, expressions, and estimation assessment criteria presented in tables and scatter plots illustrated in figures.

2.1. Cantilever Sheet Pile Walls

In the experimental investigations, the cantilever sheet pile walls rotated from a position such as O, and therefore the active and passive earth pressures switched places at the bottom of this point (Das, 2014). Figure 1 depicts the earth pressures that will occur in this situation.

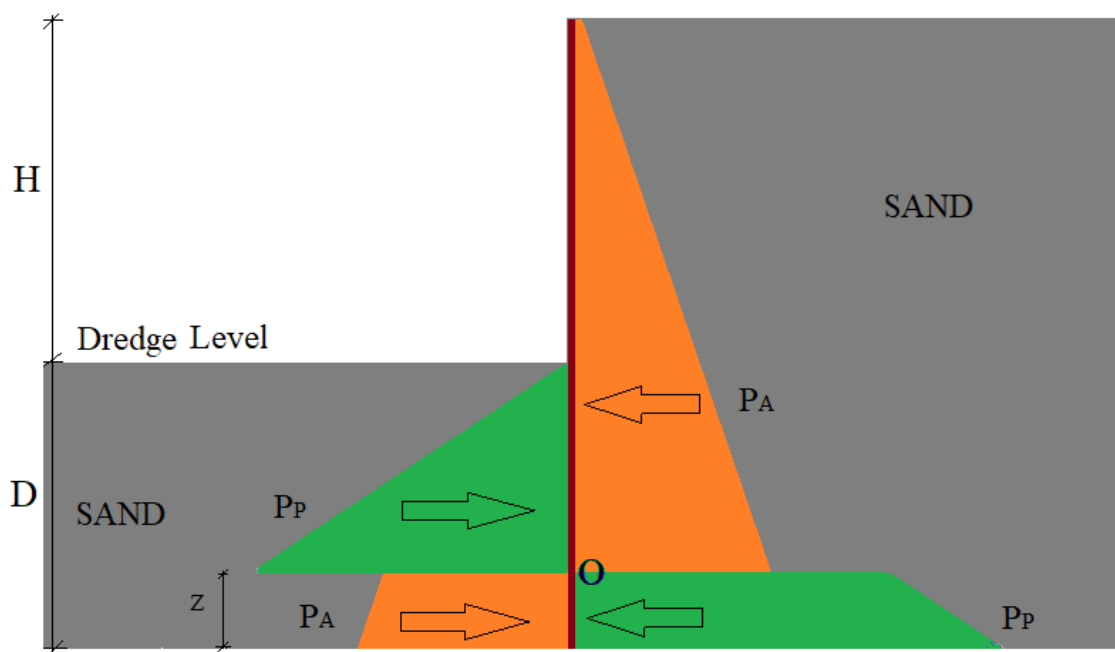


Figure 1. Lateral Earth Forces (P_A , P_P) Acting on the Cantilever Sheet Pile Wall

The approximation analytical approach was utilized to simplify the solutions. The active and passive pressure distributions behind the wall and in front of the wall are assumed to extend to the bottom of the wall in the approximation analysis, while the passive pressure behind the wall below the O point operates at the base of the wall (Sitharam, 2013). Figure 2 depicts lateral soil pressure distributions using the approximation analysis approach.

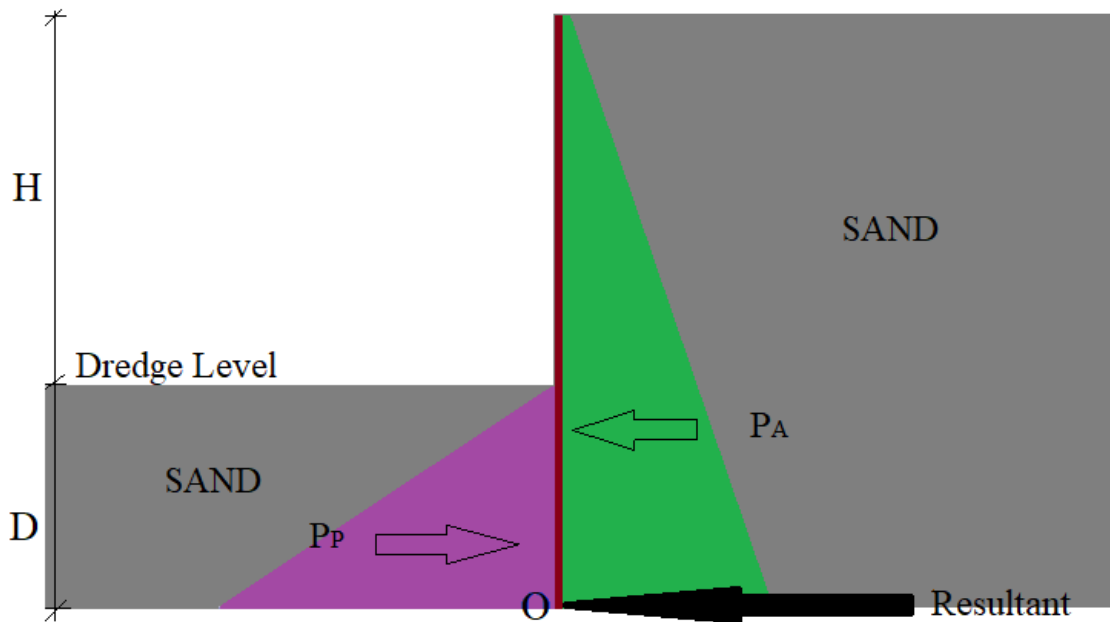


Figure 2. Lateral Earth Forces (P_A , P_P) Adopted in the Approximate Method

Rankine's theory may be used to determine the active and passive lateral earth pressure coefficients, as shown below (Rankine, 1857)(Eqs. 1-2).

$$K_a = \frac{1 - \sin(\phi)}{1 + \sin(\phi)} \tag{1}$$

$$K_p = \frac{1 + \sin(\phi)}{1 - \sin(\phi)} \tag{2}$$

where ϕ is the internal friction angle of soil. The active and passive earth pressures for cantilever sheet pile walls may be calculated using Rankine's theory. as well as the moment equilibrium achieved at the wall's base, using the following formulas (Eqs. 3-5).

$$P_a = \frac{1}{2} \gamma' (H + D)^2 K_a \tag{3}$$

$$P_p = \frac{1}{2} \gamma' D^2 K_p \tag{4}$$

$$(H + D)^3 K_a = D^3 K_p \tag{5}$$

The excavation depth is denoted by H, whereas the embedment depth is denoted by D. Equation 6 may also be used to get γ' , which is the effective unit weight of soil. The unit weight of water, γ_w , is assumed as 9.81 kN/m³ for the study purposes.

$$\gamma' = \gamma_s - \gamma_w \tag{6}$$

3.2. Model

The internal friction angle (ϕ) of the sand is raised by 1° in the range of 20° to 45°, excavation depth (H) and groundwater level (GWL, L_1) are increased by 0.5m in the ranges of 2m to 6m and 0m to 6m in the models for the solution of the Mmax, respectively. The natural unit weight of the soil above the GWL is $\gamma_n = 19$ kN/m³, whereas the saturated unit weight of the soil below the GWL is $\gamma_s = 21$ kN/m³. Figure 3 depicts a schematic illustration of the relevant model.

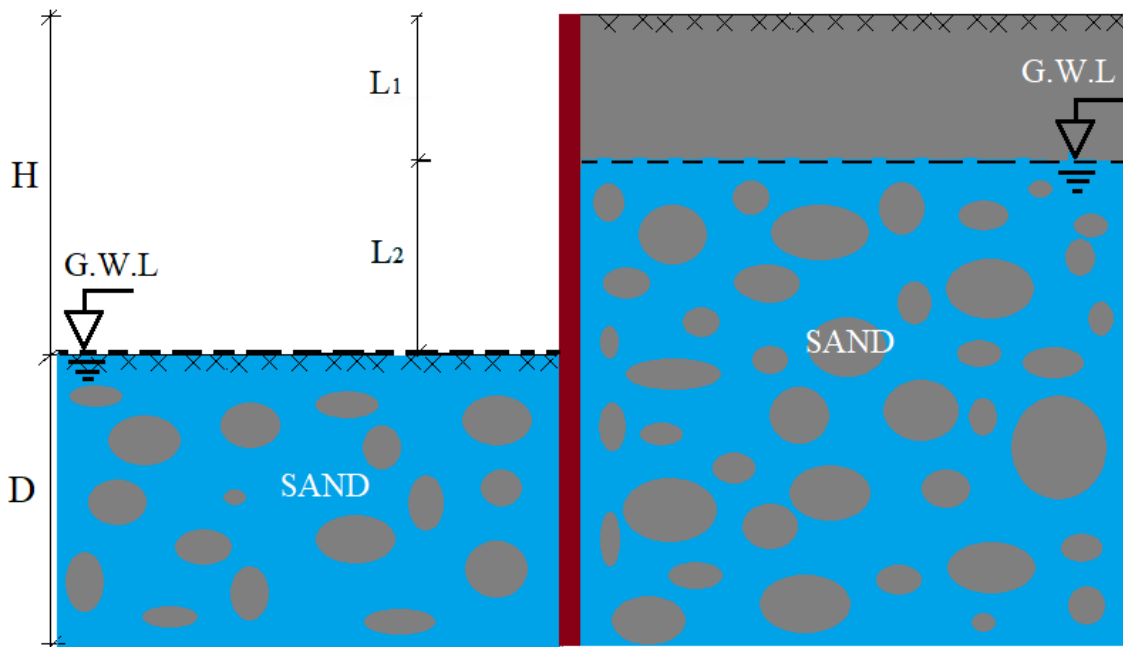


Figure 3. The Soil Profile and Cantilever Sheet Pile Wall Model

Figure 4 illustrates the active and passive lateral earth pressures, as well as the hydrostatic water pressure, that will act in the built model. The components of active earth pressure (P'_{A1} , P'_{A2} , P'_{A3} , P'_{A4} , P'_{A5}), passive earth force (P'_P), and hydrostatic water force (P_w) may be calculated using the formulas below (Eqs. 7-10).

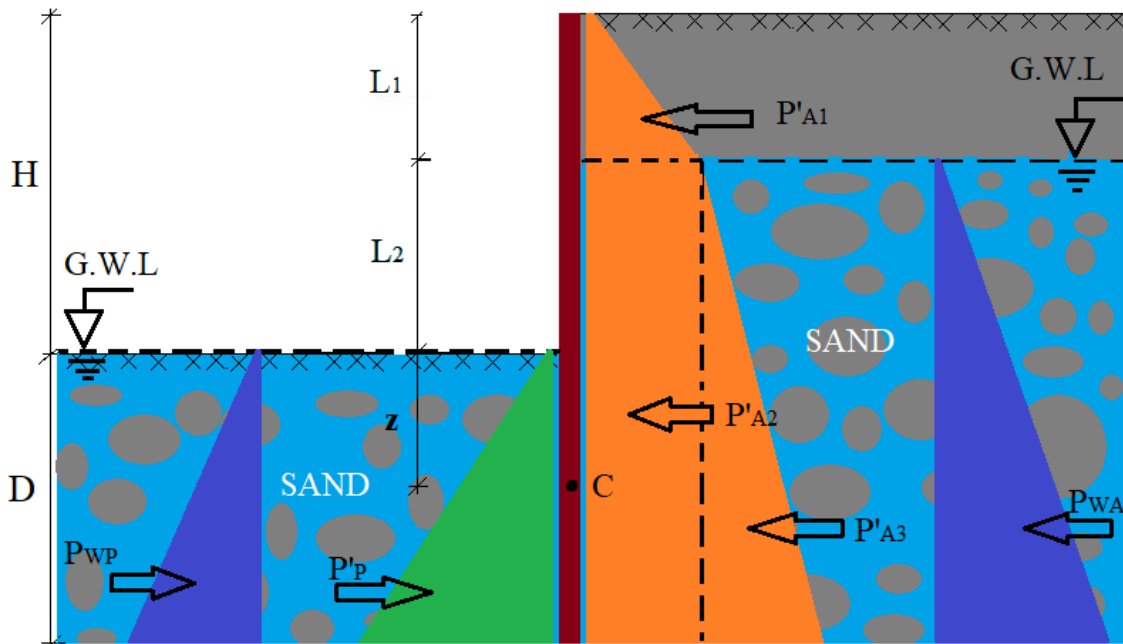


Figure 4. The Components of the Lateral Forces Acting on the Sheet Pile Wall

$$P'_{A1} = \frac{1}{2} K_a \gamma_n L_1^2 \tag{7}$$

$$P'_{A2} = \gamma_n K_a L_1 (L_2 + D) \tag{8}$$

$$P'_{A3} = \frac{1}{2} K_a \gamma' (L_2 + D)^2 \tag{9}$$

$$P'_P = \frac{1}{2} K_P \gamma' D^2 \tag{10}$$

$$P_{WA} = \frac{1}{2} \gamma_w (D + L_2)^2 \tag{11}$$

$$P_{WP} = \frac{1}{2} \gamma_w D^2 \tag{12}$$

At a depth such as z, where the forces calculated above cancel each other out horizontally, the shear force is zero and the bending moment is maximum. The following equation (Eq. 13) determines this depth, z, and the value of the moment at a point of C at this depth yields the Mmax (Eq. 14).

$$P'_{A1} + \gamma_n K_a L_1 (L_2 + z) + \frac{1}{2} K_a \gamma' (L_2 + z)^2 + \frac{1}{2} \gamma_w (z + L_2)^2 - \frac{1}{2} K_p \gamma' D z^2 - \frac{1}{2} \gamma_w z^2 = 0 \tag{13}$$

$$Mmax = P'_{A1} \left(z + L_2 + \frac{L_1}{3} \right) + \frac{1}{2} \gamma_n K_a L_1 (L_2 + z)^2 + \frac{1}{6} K_a \gamma' (L_2 + z)^3 + \frac{1}{6} \gamma_w (z + L_2)^3 - \frac{1}{6} K_p \gamma' z^3 - \frac{1}{6} \gamma_w z^3 \tag{14}$$

3.3. Multiple Linear Regression (MLR) Analysis

Regression analysis, which is extensively used in statistics, uses mathematics to anticipate linear connections between data (Olmschenk et al., 2019). An independent variable and a dependent variable have a cause-and-effect relationship in basic regression analysis (Sato-Ilic, 2017). There is one dependent variable and at least two independent variables in an MLR analysis. Simple regression analysis and MLR analysis are two types of regression analysis depending on the number of independent variables. The regression analysis method is used to investigate the impact of independent variables on the dependent variable as well as the cause-and-effect connection between them (Chantana et al., 2019; Zhang and Thomas, 2012).

A general MLR equation is as follows (Eq. 15).

$$Y = \beta_0 + \beta_1 X_1 + \beta_2 X_2 + \dots + \beta_n X_n + \varepsilon \tag{15}$$

where Y is the dependent variable, X is the independent variable, and ε is the error term in the equation.

In this paper, 833 cantilever sheet pile wall models were solved using Matlab R2015a, and the results of Mmax were analyzed by performing a step-by-step MLR analysis using SPSS Statistics v17.0. Two MLR models that have the highest R² were examined and enhanced by using polynomial functions derived from trend curves of estimated and calculated Mmax (Fig. 5-6). The dependent variable in both models is Mmax, whereas the independent variables are fi, H, L₁ in the first model and fi, Hi, L₁, and L₁H in the second. Here, fi denotes the internal friction angle (φ), H denotes the excavation depth, L₁ denotes the groundwater level (GWL), and L₁H denotes the GWL to H ratio. R² and MARE evaluate the improved and unimproved prediction performance of both models. The R² is a criterion for determining how closely variables in a regression equation are related (Polat, 2015). R² assesses a regression equation's accuracy as well as the influence of an independent variable on the dependent variable. As a result, the coefficient of determination is used to analyze the connection between dependent and independent variables in various analytic situations. In addition, MARE was utilized as a second assessment criterion to measure the estimating success of the produced expressions, which determines the percent difference between estimated and calculated Mmax outcomes using the equation below (Eq. 16).

$$MARE = \frac{1}{n} \sum_{t=1}^n \left| \frac{T_t - H_t}{H_t} \right| * 100 \tag{16}$$

- n : Number of data evaluated
- T_t : Estimated value
- H_t : Calculated value

4. Results

Table 1 displays the variables and the adjusted R² of various models while Table 2 displays the MLR equations, R², and MARE of Model 3 and Model 4 which have the highest R². As shown in Table 1, model 4 using fi, H, L₁, and L₁H as variables produces the best results among the models developed to predict the Mmax. Models 3 and 4, which are the best two models were investigated in this study, and the findings are shown in Figs. 5-6 and Table 2.

Table 1. Results of MLR Analysis

Model	Independent Variables	R	R Square	Adjusted R Square
1	H	.703	.495	.494
2	H-fi	.834	.695	.694
3	H-fi-L ₁	.920	.847	.846
4	H-fi-L ₁ -L ₁ H	.933	.871	.871

Model 3, which is developed by adding the L1 variable to the fi and H variables, has a 22 percent improvement in R² when compared to Model 2. Similarly, the R² value of Model 4 developed by adding the L₁H variable to Model 3 increased by 3% when compared to Model 3 when the MARE decreased about 13% (Table 2). This demonstrates that all variables have a substantial influence on estimating Mmax.

Table 2. Equations and Variables of MLR Model 3 and Model 4

Model	Independent Variables	The equation obtained from MLR analysis (x)	MARE (%)	R ²
3	H-fi-L ₁	$M_{max}=637.290+342.487*H-39.814*fi -146.584*L_1$	75.359	.846
4	H-fi-L ₁ -L ₁ H	$M_{max}=-379.723+542.429*H-39.814*fi -424.294*L_1+1400.452* L_1H$	65.577	.871

Model 3 has adjusted R² of 0.846 and MARE of 75.359%, whereas Model 4 has adjusted R² 0.871 and MARE of 65.577% (Table 2). Figures 5 and 6 depict the dispersion of theoretically computed values versus estimated values derived from the regression equations of Model 3 and Model 4.

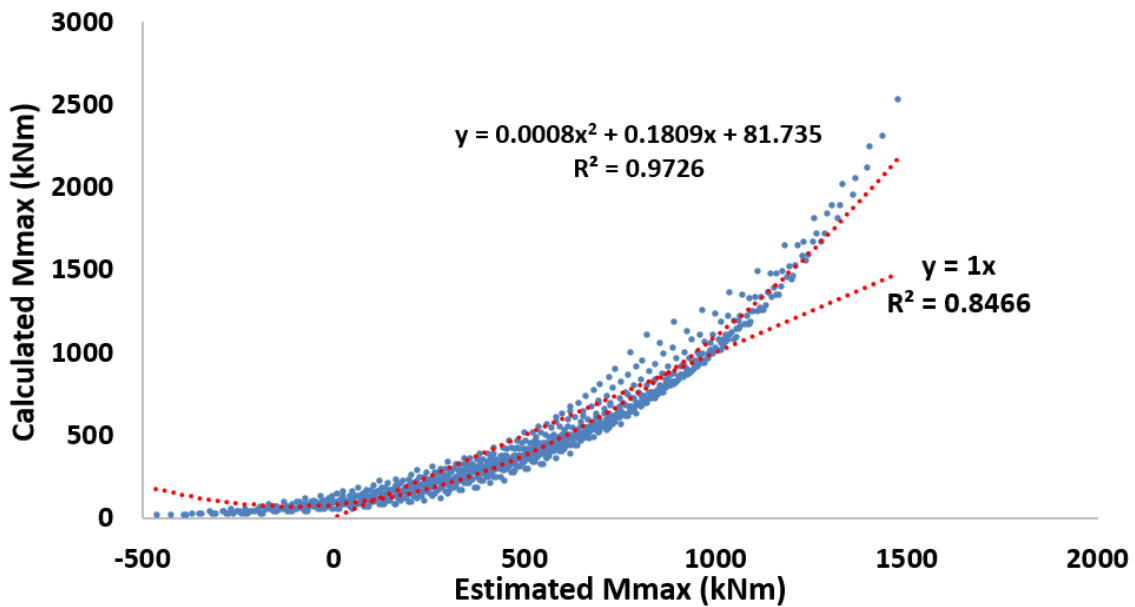


Figure 5. Scatter of Estimated and Calculated Mmax Results of Model 3

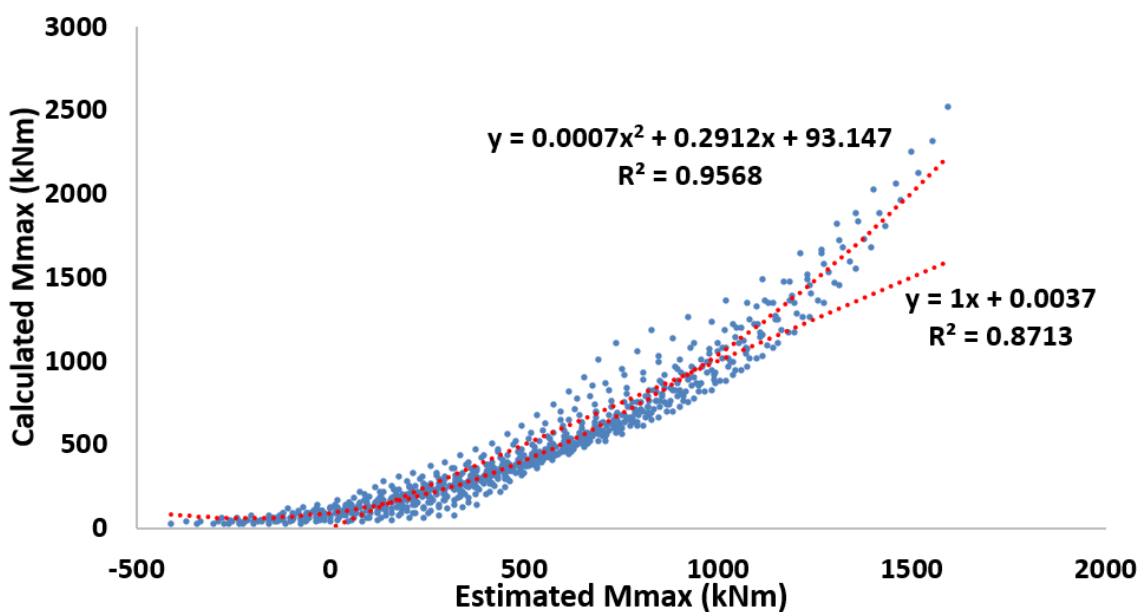


Figure 6. Scatter of Estimated and Calculated Mmax Results of Model 4

Figures 5-6 include a polynomial curve that depicts the connection between computed and estimated Mmax values. The Mmax values predicted by the MLR equations are employed as a variable in the equation of this polynomial curve and the accuracy of the calculation is enhanced. The R² and MARE values of these polynomial equations and the improved predictive values obtained with them are shown in Table 3, and scatter diagrams of the calculated values and the improved predictive values are shown in Figures 7-8.

Table 3. Polynomial Equations for Improving the Results of the Mmax of Model 3 and Model 4

Model	Polynomial Equations	MARE (%)	R ²
3	$0.0008x^2 + 0.1809x + 81.735$	20.622	0.979
4	$0.0007x^2 + 0.2912x + 93.147$	22.005	0.949

The R² increases from 0.846 to 0.979 for Model 3 and from 0.871 to 0.949 for Model 4 with the help of the polynomial equation, while the MARE decreases from 75.359 to 20.622 and from 65.577 to 22.005, respectively. It is shown that Model 3 increases the prediction success by 16% based on R² and 73% based on MARE, while the prediction success of Model 4 increases by 9% based on R² and 66% based on MARE.

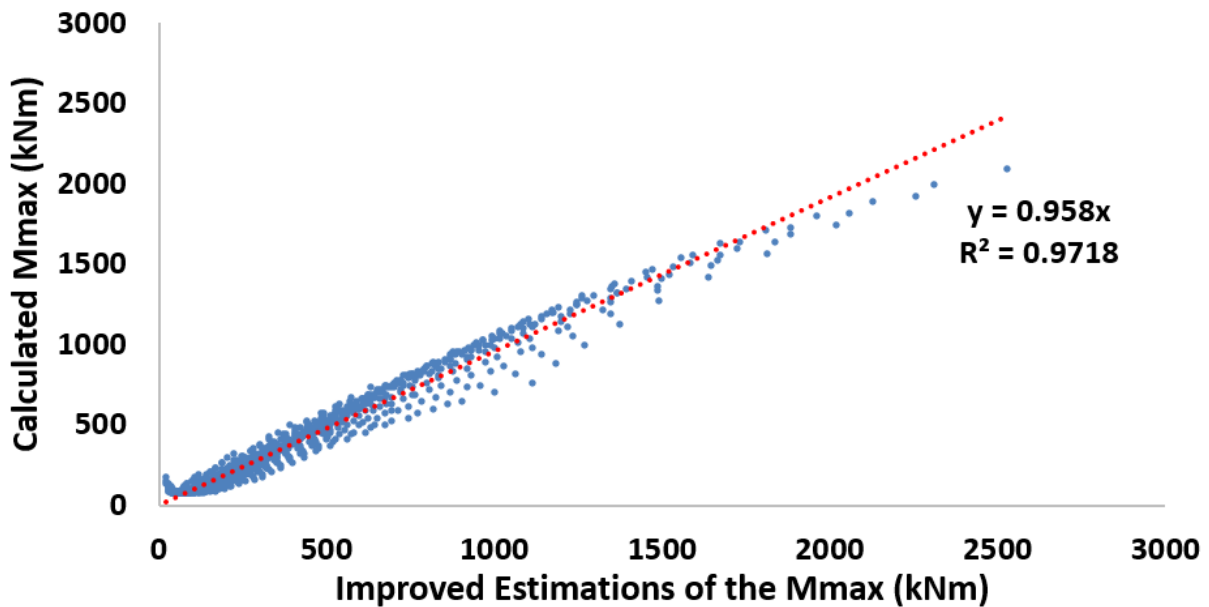


Figure 7. Scatter of Improved Estimations and Calculated Results of the Mmax of Model 3

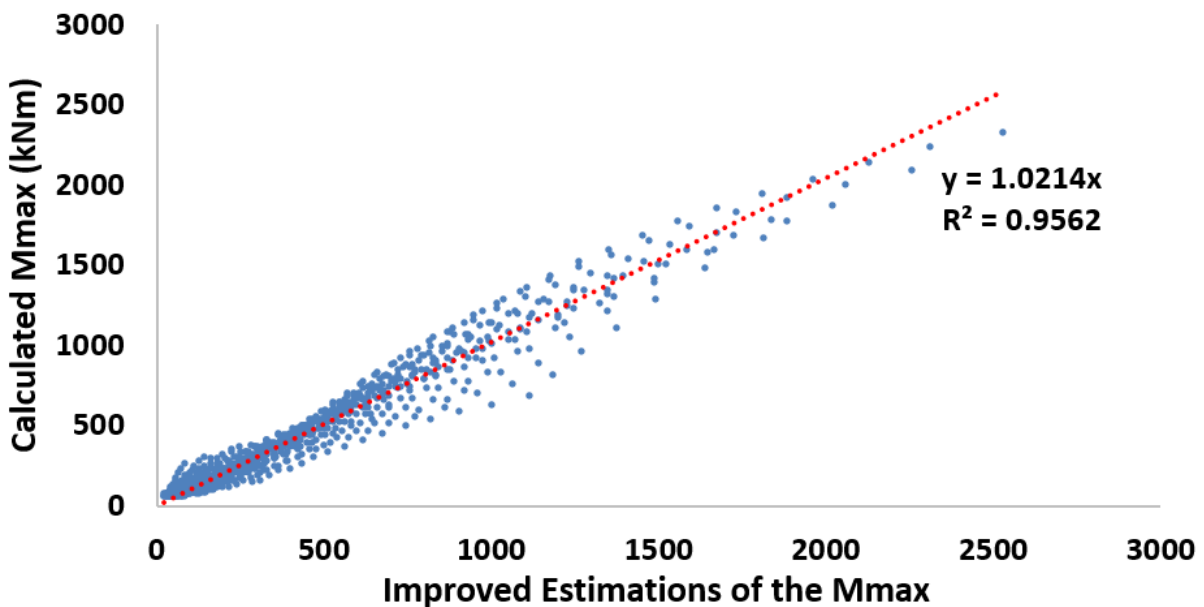


Figure 8. Scatter of Improved Estimations and Calculated Results of the Mmax of Model 4

The adjusted R^2 of the polynomial equation recommended for Model 3 is 0.979 while the MARE is 20.622% and the adjusted R^2 of the polynomial equation recommended for Model 4 is 0.949 while the MARE is 22.005%. Although both models have the satisfying predictive capability with the help of polynomial equations it is seen that Model 3 provides more successful prediction than Model 4.

5. Conclusion

The M_{max} that will occur in the cross-section of a cantilever sheet pile wall is calculated in this work using expressions acquired from MLR analysis, which simplifies the calculation procedure. For his aim, a cantilever sheet pile wall was driven into a sandy soil with the groundwater level at the dredge line in front and at various levels from the soil surface to the dredge line rear of the wall was modeled with the aid of Matlab R2015a. Then the obtained M_{max} results are subjected to MLR analysis with the help of SPSS Statistics v17.0 and MLR expressions to estimate the M_{max} are generated. Accordingly, the following conclusions can be drawn:

- The best model established to determine the M_{max} has R^2 of 0.846 and MARE of 75.359%. This is an unsuccessful result for the estimation of the M_{max} by the MLR analysis.
- The M_{max} in the cantilever sheet pile wall, can be estimated by using linear MLR models with an enhancement by polynomial equations with R^2 of 0.98 and MARE of 20.6.
- It is shown that Model 3 increases the prediction success by 16% based on R^2 and 73% based on MARE.
- The best model to predict the M_{max} has internal friction angle of sand, groundwater level, and excavation depth as independent variables.
- All the results and conclusions presented in the study, include the study-specific soil profile and sheet pile wall design conditions. In order to be generalized, it needs to be expanded by further studies.

Conflict of Interest

No conflict of interest was declared by the author.

References

- Abdi, Y., Garavand, A.T., Sahamieh, R.Z., 2018. Prediction of strength parameters of sedimentary rocks using artificial neural networks and regression analysis. *Arab. J. Geosci.* 2018 1119 11, 1–11. <https://doi.org/10.1007/S12517-018-3929-0>
- Adefemi, B.A., Wole, A.C., 2013. Regression Analysis of Compaction Delay on CBR and UCS of Lime Stabilized Yellowish Brown Lateritic Soil. *EJGE* 18, 3301–3314.
- Akbar, Z., Dalyan, İ., Akin, M.S., Gençdal, H.B., 2020. An Application of TBEC-2018 in the Prediction of Retaining Wall Dimensions with Simple Regression Analysis. *Glob. J. Civ. Eng.* 2.
- Azzouz, A.S., Krizek, R.J., Corotis, R.B., 1976. Regression Analysis of Soil Compressibility. *Soils Found.* 16, 19–29. https://doi.org/10.3208/SANDF1972.16.2_19
- Bera, A.K., Ghosh, Ambarish, Ghosh, Amalendu, 2005. Regression model for bearing capacity of a square footing on reinforced pond ash. *Geotext. Geomembranes* 23, 261–285. <https://doi.org/10.1016/J.GEOTEXMEM.2004.09.002>
- Bolton, M.D., Powrie, W., Symons, I.F., 1990a. The design of stiff in-situ walls retaining over consolidated clay-Part II: short-term behaviour (continued). *Gr. Eng.* 22, 34–40.
- Bolton, M.D., Powrie, W., Symons, I.F., 1990b. The design of stiff in-situ walls retaining over consolidated clay-Part II: long-term behaviour (continued). *Gr. Eng.* 23, 22–28.
- Bolton, M.D., Powrie, W., Symons, I.F., 1989. The design of stiff in-situ walls retaining over consolidated clay-Part I: short-term behaviour. *Gr. Eng.* 22, 44–47.
- Bransby, J.E., Milligan, G.W.E., 1975. Soil Deformations near Cantilever Retaining Walls. *Geotechnique* 24, 175–195.
- Chantana, J., Kawano, Y., Kamei, A., Minemoto, T., 2019. Description of degradation of output performance for photovoltaic modules by multiple regression analysis based on environmental factors. *Optik (Stuttg.)*. 179, 1063–1070. <https://doi.org/10.1016/J.IJLEO.2018.11.040>
- Choi, M., Lee, G., 2010. Decision tree for selecting retaining wall systems based on logistic regression analysis. *Autom. Constr.* 19, 917–928. <https://doi.org/10.1016/J.AUTCON.2010.06.005>
- Choudry, D., Singh, S., Goel, S., 2006. New approach for analysis of cantilever sheet pile with line load. *J. Geotech. Geoenvironmental Eng.* 43, 540–549.
- Coduto, D.P., 2001. *Foundation Design: Principles and Practices*. Prentice Hall, New Jersey, USA.
- Dagdeviren, U., Kaymak, B., 2020. A regression-based approach for estimating preliminary dimensioning of reinforced concrete cantilever retaining walls. *Struct. Multidiscip. Optim.* 61, 1657–1675. <https://doi.org/10.1007/s00158-019-02470-w>
- Das, B.M., 2014. *Principles of Foundation Engineering*. Cengage Learning, Boston, MA, USA.
- Das, B.M., 2007. *Principles of Foundation Engineering*, 6th Edition. Brooks/Cole Publishing Company, Pacific Grove, CA.
- Gajan, S., 2011. Normalized Relationships for Depth of Embedment of Sheet Pile Walls and Soldier Pile Walls in Cohesionless Soils. *Soils Found.* 51, 559–564. <https://doi.org/10.3208/SANDF.51.559>
- Hagerty, D.J., Nofal, M.M., 1992. Design aids-anchored bulkheads in sand. *Can. Geotech. J.* 29, 789–795.
- Hirata, S., Yao, S., Nishida, K., 1990. MULTIPLE REGRESSION ANALYSIS BETWEEN THE MECHANICAL AND PHYSICAL PROPERTIES OF COHESIVE SOILS. *SOILS Found.* 30, 91–108. https://doi.org/10.3208/SANDF1972.30.3_91

- Mahdiabadi, N., Khanlari, G., 2019. Prediction of Uniaxial Compressive Strength and Modulus of Elasticity in Calcareous Mudstones Using Neural Networks, Fuzzy Systems, and Regression Analysis. *Period. Polytech. Civ. Eng.* 63, 104–114. <https://doi.org/10.3311/PPCI.13035>
- Olmschenk, G., Zhu, Z., Tang, H., 2019. Generalizing semi-supervised generative adversarial networks to regression using feature contrasting. *Comput. Vis. Image Underst.* 186, 1–12. <https://doi.org/10.1016/j.cviu.2019.06.004>
- Polat, Ö., 2015. A robust regression based classifier with determination of optimal feature set. *J. Appl. Res. Technol.* JART 13, 443–446. <https://doi.org/10.1016/J.JART.2015.08.001>
- Rankine, W.J., 1857. II. On the stability of loose earth. *Philos. Trans. R. Soc. London* 147, 9–27.
- Rowe, P.W., 1952. Anchored Sheet-pile walls. *Proc. Inst. Civ. Eng.* 1, 27–70. <https://doi.org/10.1680/iicep.1952.10942>
- Rowe, P.W., 1951. Cantilever sheet piling in cohesionless soil, in: *Engineering. Institution of Civil Engineer, London, England*, pp. 316–319.
- Sato-Ilic, M., 2017. Knowledge-based Comparable Predicted Values in Regression Analysis. *Procedia Comput. Sci.* 114, 216–223. <https://doi.org/10.1016/J.PROCS.2017.09.063>
- Seok, J.W., Kim, O.Y., Chung, C.K., Kim, M.M., 2001. Evaluation of ground and building settlement near braced excavation sites by model testing. *Can. Geotech. J.* 38, 1127–1133. <https://doi.org/10.1139/CGJ-38-5-1127>
- Sitharam, T.G., 2013. *Advanced Foundation Engineering*. Indian Institute of Science, Bangalore, India.
- Srivastava, A., Malhotra, M., 2016. Earth Pressure behind a Retaining Wall under Linearly Varying Geotechnical Parameters. *Indian J. Sci. Technol.* 9, 1–8. <https://doi.org/10.17485/IJST/2016/V9IS1/105809>
- Teymen, A., Mengüç, E.C., 2020. Comparative evaluation of different statistical tools for the prediction of uniaxial compressive strength of rocks. *Int. J. Min. Sci. Technol.* 30, 785–797. <https://doi.org/10.1016/J.IJMST.2020.06.008>
- Yoon, G.L., Kim, B.T., 2006. Regression Analysis of Compression Index for Kwangyang Marine Clay. *KSCE J. Civ. Eng.* 10, 415.
- Yoon, S., Lee, S.R., Kim, Y.T., Go, G.H., 2015. Estimation of saturated hydraulic conductivity of Korean weathered granite soils using a regression analysis. *Geomech. Eng.* 9, 101–113. <https://doi.org/10.12989/GAE.2015.9.1.101>
- Zhang, J., Thomas, L.C., 2012. Comparisons of linear regression and survival analysis using single and mixture distributions approaches in modelling LGD. *Int. J. Forecast.* 28, 204–215. <https://doi.org/10.1016/J.IJFORECAST.2010.06.002>